J|A|C|S
ARTICLES
Published on Web 04/23/2004

Conformational Analysis and Assignments of Relative Stereocenter Configurations in Fluoroalkyl−Iridium Complexes Using $^{19}F\{^1H\}$ HOESY Experiments. Comparison with Solid-State X-ray Structural Results

Russell P. Hughes,*,† Donghui Zhang,† Antony J. Ward,† Lev. N. Zakharov,‡ and Arnold L. Rheingold‡

Contribution from the Departments of Chemistry, 6128 Burke Laboratory, Dartmouth College, Hanover, New Hampshire 03755, and University of California, San Diego, California 92093-0358

Received February 12, 2004; E-mail: rph@dartmouth.edu

Abstract: Solution conformations about the metal−carbon bond of the secondary fluoroalkyl ligands in iridium complexes [IrCp*(PMe$_3$)(R$_F$)X] [Cp* = C$_5$Me$_5$; R$_F$ = CF(CF$_3$)$_2$, X = I (**1**), CH$_3$ (**2**); R$_F$ = CF(CF$_3$)(CF$_2$CF$_3$), X = I (**4**), CH$_3$ (**5**)] have been determined using $^{19}F\{^1H\}$ HOESY techniques. The molecules adopt the staggered conformation with the tertiary fluorine in the more hindered sector between the PMe$_3$ and X ligands, with CF$_3$ (and CF$_2$CF$_3$) substituents lying in the less hindered regions between PMe$_3$ and Cp* or X and Cp*. In molecules containing the CF(CF$_3$)$_2$ ligand, these conformations are identical to those adopted in the solid state. For compound **4**, containing the CF(CF$_3$)(CF$_2$CF$_3$) ligand, two diastereomers are observed in solution. Solution conformations and relative stereocenter configuration assignments have been obtained using $^{19}F\{^1H\}$ HOESY and correlated with the X-ray structure for the major diastereomer of **4**, which has the (S_{Ir}, S_C) or (R_{Ir}, R_C) configuration. Relative stereocenter configurations of analogue **5**, for which no suitable crystals could be obtained, were assigned using $^{19}F\{^1H\}$ HOESY and proved to be different from **4**, with **5** preferring the (S_{Ir}, R_C) or (R_{Ir}, S_C) configuration.

Introduction

The observation of nuclear Overhauser effects (nOe) by two-dimensional homonuclear $^1H\{^1H\}$ magnetic resonance is a powerful and widely used method in studying solution structures and conformations of biological molecules. For molecules bearing protons and fluorinated groups, two-dimensional $^{19}F\{^1H\}$ HOESY (heteronuclear Overhauser effect spectroscopy) techniques also provide detailed information in solution about the relative spatial orientation of groups containing protons and fluorines, with a cross-peak observed if two nuclei are close in space (≤5 Å).[1] It has been extensively used in studying transition metal ion-pair interactions in solution,[2−20] time averaged ion-pair structures of organic salts,[21] and interactions of ^{19}F-labeled substrates with proteins at the active sites.[22,23] We have used this technique to determine the conformations and relative proximities of fluorine substituents in aryl ligands to neighboring phosphines,[24,25] but we are unaware of any applications of this technique in the determination of intramo-

† Dartmouth College.
‡ University of California, San Diego.

(1) Neuhaus, D.; Williamson, M. P. *The Nuclear Overhauser Effect in Structural and Conformational Analysis*, 2nd ed.; Wiley-VCH: New York, 2000.
(2) Macchioni, A.; Magistrato, A.; Orabona, I.; Ruffo, F.; Rothlisberger, U.; Zuccaccia, C. *New J. Chem.* **2003**, *27*, 455−458.
(3) Macchioni, A.; Romani, A.; Zuccaccia, C. *Organometallics* **2003**, *22*, 1526−1533.
(4) Macchioni, A. *Eur. J. Inorg. Chem.* **2003**, 195−205.
(5) Kumar, P. G. A.; Pregosin, P. S.; Goicoechea, J. M.; Whittlesey, M. K. *Organometallics* **2003**, *22*, 2956−2960.
(6) Drago, D.; Pregosin, P. S.; Pfaltz, A. *Chem. Commun.* **2002**, 286−287.
(7) Burini, A.; Fackler, J. P.; Galassi, R.; Macchioni, A.; Omary, M. A.; Rawashdeh-Omary, M. A.; Pietroni, B. R.; Sabatini, S.; Zuccaccia, C. *J. Am. Chem. Soc.* **2002**, *124*, 4570−4571.
(8) Binotti, B.; Bellachioma, G.; Cardaci, G.; Macchioni, A.; Zuccaccia, C. *Organometallics* **2002**, *21*, 346−354.
(9) Bellachioma, G.; Binotti, B.; Cardaci, G.; Carfagna, C.; Macchioni, A.; Sabatini, S.; Zuccaccia, C. *Inorg. Chim. Acta* **2002**, *330*, 44−51.
(10) Zuccaccia, C.; Bellachioma, G.; Cardaci, G.; Macchioni, A. *J. Am. Chem. Soc.* **2001**, *123*, 11020−11028.
(11) Romeo, R.; Fenech, L.; Scolaro, L. M.; Albinati, A.; Macchioni, A.; Zuccaccia, C. *Inorg. Chem.* **2001**, *40*, 3293−3302.
(12) Goumain, S.; Oulyadi, H.; Jubault, P.; Feasson, C.; Quirion, J.-C. *J. Chem. Soc., Perkin Trans. 1* **2001**, 701−705.
(13) Bellachioma, G.; Cardaci, G.; D'Onofrio, F.; Macchioni, A.; Sabatini, S.; Zuccaccia, C. *Eur. J. Inorg. Chem.* **2001**, 1605−1611.
(14) Bellachioma, G.; Cardaci, G.; Macchioni, A.; Zuccaccia, C. *J. Organomet. Chem.* **2000**, *593*−*594*, 119−126.
(15) Bellachioma, G.; Cardaci, G.; Macchioni, A.; Valentini, F.; Zuccaccia, C.; Foresti, E.; Sabatino, P. *Organometallics* **2000**, *19*, 4320−4326.
(16) Bachechi, F.; Burini, A.; Galassi, R.; Macchioni, A.; Pietroni, B. R.; Ziarelli, F.; Zuccaccia, C. *J. Organomet. Chem.* **2000**, *593*−*594*, 392−402.
(17) Zuccaccia, C.; Macchioni, A.; Orabona, I.; Ruffo, F. *Organometallics* **1999**, *18*, 4367−4372.
(18) Macchioni, A.; Bellachioma, G.; Cardaci, G.; Travaglia, M.; Zuccaccia, C.; Milani, B.; Corso, G.; Zangrando, E.; Mestroni, G.; Carfagna, C.; Formica, M. *Organometallics* **1999**, *18*, 3061−3069.
(19) Romeo, R.; Nastasi, N.; Scolaro, L. M.; Plutino, M. R.; Albinati, A.; Macchioni, A. *Inorg. Chem.* **1998**, *37*, 5460−5466.
(20) Macchioni, A.; Bellachioma, G.; Cardaci, G.; Gramlich, V.; Rueegger, H.; Terenzi, S.; Venanzi, L. M. *Organometallics* **1997**, *16*, 2139−2145.
(21) Hofstetter, C.; Pochapsky, T. C. *Magn. Reson. Chem.* **2000**, *38*, 90−94.
(22) Hammond, S. J. *J. Chem. Soc., Chem. Commun.* **1984**, 712−713.
(23) Cistola, D. P.; Hall, K. B. *J. Biomol. NMR* **1995**, *5*, 415−419.
(24) Hughes, R. P.; Laritchev, R. B.; Williamson, A.; Incarvito, C. D.; Zakharov, L. N.; Rheingold, A. L. *Organometallics* **2003**, *22*, 2134−2141.
(25) Hughes, R. P.; Laritchev, R. B.; Williamson, A.; Incarvito, C. D.; Zakharov, L. N.; Rheingold, A. L. *Organometallics* **2002**, *21*, 4873−4885.

lecular conformations in organometallic systems involving fluoroaliphatic ligands. In view of our recent results on the activation of α-CF bonds in fluoroalkyl complexes of iridium,[26−28] we have been interested in determining the preferred solution conformations of the fluoroalkyl ligands in these compounds. Here, we describe application of the $^{19}F\{^1H\}$ HOESY technique to the determination of the solution conformations and, where applicable, the assignment of relative diastereomeric stereocenter configurations in complexes containing secondary fluoroalkyl ligands.

Results and Discussion

The compounds of interest here are all prepared using the general methodology of oxidative addition of a fluoroalkyl iodide (R_FI) to $Cp^*Ir(CO)_2$ to give $Cp^*Ir(CO)(R_F)I$, followed by replacement of CO by PMe_3 to afford $Cp^*Ir(PMe_3)(R_F)I$. The synthesis and solid-state molecular structures of perfluoro-iso-propyl compound **1** have been reported previously.[29] Conversion to the corresponding methyl compound **2** can be achieved via methylation of an intermediate triflate compound $Cp^*Ir(PMe_3)(R_F)OT_F$ using excess MeLi, as reported previously for a primary fluoroalkyl analogue.[26] Reaction with 1 equiv of $ZnMe_2$ at low temperatures gives about 80% yield of **2**, while use of excess $ZnMe_2$ results in complex mixtures of products. The best method involves alkylation using 0.5 equiv of Cp_2ZrMe_2 at room temperature to afford **2** quantitatively. It is important to replace iodide (or bromide or chloride) on Ir with triflate prior to alkylation, as the halo compounds do not alkylate under these conditions. Consequently, it is also important to use halide free alkylating agents; Grignard reagents or halide-containing methyllithium solutions rapidly convert the intermediate Ir−triflate to the halide complex, which is then inert to methylation. Compound **2** has been characterized spectroscopically and by a single-crystal X-ray diffraction study.

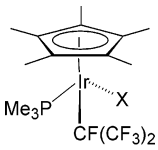

1. X = I
2. X = CH_3

The methyl complex **2** displays characteristic Cp* and PMe_3 peaks in the ^1H NMR spectrum. In C_6D_6, the CH_3 group appears as a doublet of quartet of doublets at 0.66 ppm from coupling with ^{31}P, one CF_3, and the α-fluorine. In the ^{19}F NMR spectrum, **2** exhibits two mutually coupled resonances at −69.3 and −69.9 ppm due to the two diastereotopic CF_3 groups, with the one at lower field (−69.3 ppm) also showing additional coupling to the α-fluorine. The higher field CF_3 (−69.9 ppm) appears as a doublet of quartets of doublets of quartets from coupling with the α-fluorine, the other CF_3, ^{31}P, and the CH_3. The α-fluorine resonates at −179.6 ppm as a broad singlet due to the complicated coupling with the two CF_3 groups as well as ^{31}P. The corresponding $^{31}P\{^1H\}$ spectrum exhibits a doublet of quartets from coupling with the α-fluorine and the higher field CF_3 (−69.9 ppm). Compound **2** was also characterized by a single-crystal X-ray diffraction experiment; an ORTEP representation of the structure, along with representative bond lengths and angles, is shown in Figure 1. Details of the structural determination are provided in Table 1.

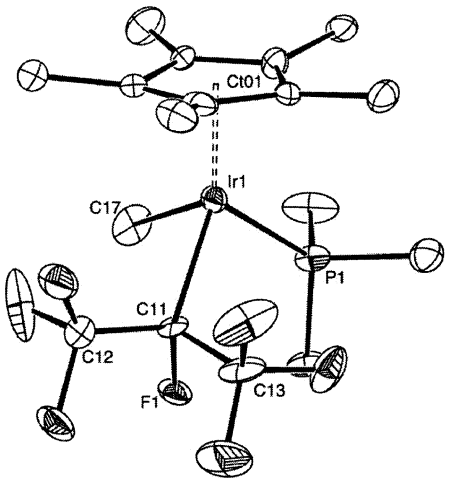

Figure 1. ORTEP diagram of the non-hydrogen atoms of **2**, showing the partial atom-labeling scheme. Thermal ellipsoids are shown at the 30% level. Selected bond lengths (Å) and angles (deg): Ir(1)−C(17), 2.22(2); Ir(1)−C(11), 2.150(16); Ir(1)−Ct01, 1.9162(5); Ir(1)−P(1), 2.258(4); C(11)−F(1), 1.429(15); Ct01−Ir(1)−C(17), 120.0(6); Ct01−Ir(1)−C(11), 129.6(4); Ct01−Ir(1)−P(1), 127.48(11); Ir(1)−C(11)−C(12), 116.0(10); Ir(1)−C(11)−C(13), 113.30(11); Ir(1)−C(11)−F(1), 112.00(12); C(11)−Ir(1)−P(1), 94.1(4); C(11)−Ir(1)−C(17), 87.0(7); C(17)−Ir(1)−P(1), 83.5(5).

The three staggered conformations of complexes **1** and **2** are viewed in Figure 2, as Newman projections looking down the C−Ir bond of the fluoroalkyl ligand. The 15 protons of a rapidly rotating pentamethylcyclopentadienyl (Cp*) ligand, and the nine protons of a likewise rapidly rotating PMe_3 ligand, provide two spatial reference points; in compounds where X = CH_3, the three methyl protons provide information about the third sector of space around iridium. Based on the known solid-state structure of a number of such piano-stool complexes of Ir, it is clear that the three spatial zones around Ir between the Cp*, PMe_3, and X ligands should have quite different abilities to accommodate the steric requirements of the individual components of the fluoroalkyl ligand. The acute P−Ir−I angle of approximately 85° contrasts with the far more obtuse angles between I (120°) or PMe_3 (125°) and the Cp* centroid and suggests that the former zone is likely to be more sterically crowded than the latter two.[29] This prediction is borne out by the observed structures of **1**[29] and **2**, which favor conformation A.

Compounds **1**[29] and **2**, for which the solid-state structures are known, were chosen as the simplest tests of the applicability of the HOESY technique to the determination of solution conformations. No attempts were made to use this technique to measure specific distances as others have done;[4,10] this is far more time-consuming, and here we are concerned only with determining relative proximities closely enough to afford a rapid, yet unambiguous determination of solution conformation or relative configuration.

The $^{19}F\{^1H\}$ HOESY spectrum obtained for **1** is shown in Figure 3. The following observations can be made from the

(26) Hughes, R. P.; Zhang, D.; Zakharov, L. N.; Rheingold, A. L. *Organometallics* **2002**, *21*, 4902−4904.
(27) Hughes, R. P.; Willemsen, S.; Williamson, A.; Zhang, D. *Organometallics* **2002**, *21*, 3085−3087.
(28) Hughes, R. P.; Smith, J. M. *J. Am. Chem. Soc.* **1999**, *121*, 6084−6085.
(29) Hughes, R. P.; Smith, J. M.; Liable-Sands, L. M.; Concolino, T. E.; Lam, K.-C.; Incarvito, C.; Rheingold, A. L. *J. Chem. Soc., Dalton Trans.* **2000**, 873−879.

Table 1. Crystal, Data Collection, and Refinement Parameters

compound	**2**	**3**	**4**
formula	$C_{17}H_{27}F_7PIr$	$C_{15}H_{15}F_9O_3IIr$	$C_{17}H_{24}F_9PIIr$
formula weight	587.56	701.37	749.43
space group	$P2_12_12_1$	$P2_1/n$	Cc
a, Å	9.4733(4)	8.5210(7)	9.4637(7)
b, Å	11.9166(5)	15.2085(12)	15.4169(7)
c, Å	17.5861(8)	14.6563(12)	14.9804(9)
α, deg			
β, deg		95.585(2)	90.160(2)
γ, deg			
V, Å^3	1985.29(15)	1890.3(3)	2185.6(2)
Z	4	4	4
crystal color, habit	colorless, block	orange/yellow, plate	orange/yellow, block
D (calc), g cm^{-3}	1.966	2.464	2.278
μ (Mo Kα), mm^{-1}	6.87	8.78	7.67
temp, K	100(2)	173(2)	173(2)
diffractometer	Bruker Smart Apex CCD	Siemens P4 CCD	Siemens P4 CCD
radiation	Mo Kα ($\lambda = 0.71073$ Å)	Mo Kα ($\lambda = 0.71073$ Å)	Mo Kα ($\lambda = 0.71073$ Å)
measured reflns	9127	9099	5251
independent reflns	2932 [$R_{int} = 0.0371$]	4029 [$R_{int} = 0.0638$]	3485 [$R_{int} = 0.0514$]
R (F), %[a]	5.07	4.50	3.64
R (wF^2),%[b]	11.75	12.14	9.57

[a] $R = \sum||F_o| - |F_c||/\sum|F_o|$. [b] $R(\omega F^2) = \{\sum[\omega(F_o^2 - F_c^2)^2]/\sum[\omega(F_o^2)^2]\}^{1/2}$; $\omega = 1/[\sigma^2(F_o^2) + (aP)^2 + bP]$, $P = [2F_c^2 + \max(F_o,0)]/3$.

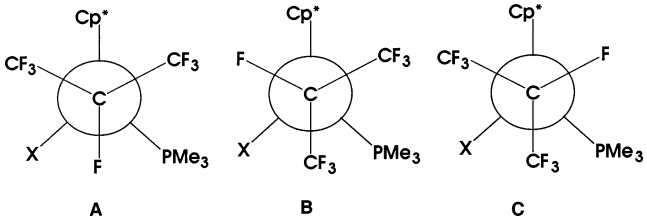

Figure 2. Newman projections, viewed down the C−Ir bond, of the three staggered conformations of complexes **1** and **2**.

observed cross-peaks: one of the diastereotopic trifluoromethyl groups, CF_3^A, is close in space to both Cp* and PMe_3; the other, CF_3^B, is close to Cp* only; the tertiary F_A is close in space to PMe_3 only. The only solution conformation consistent with these observations is shown in Figure 4, using a Newman projection, along with an ORTEP representation of the previously determined crystal structure for this complex, both viewed along the α-C_F−Ir bond.[29] Clearly, the preferred solution conformation is the same as that observed in the solid state. As expected, the more sterically crowded P−Ir−I sector accommodates F rather than the more sterically demanding CF_3.

Notably, in the one-dimensional $^{31}P\{^1H\}$ NMR spectrum of **1**, the PMe_3 signal appears as a doublet of quartets from coupling with the tertiary F_A and only the CF_3 identified by the HOESY experiment as CF_3^A, which is closer in space to PMe_3. As observed previously for fluoroaryl ligands,[24,25] larger values of J_{PF} are observed at shorter P−F distances in these types of complexes.

In complex **1**, the iodide ligand is NMR silent and a nonreporter for the zone in which it lies. The $^{19}F\{^1H\}$ HOESY spectrum for the analogous methyl complex **2** is shown in Figure 5. From the $^{19}F\{^1H\}$ HOESY spectrum, analogous qualitative observations can be made: one CF_3^A is close in space to both Cp* and PMe_3; the other CF_3^B is close to both Cp* and CH_3; the tertiary F_A is close in space to both PMe_3 and CH_3. These observations are presented graphically in Figure 6, using a Newman projection and an ORTEP view of the crystal structure for **2**, each viewed along the α-C_F−Ir bond. Clearly, the solution conformation is again that observed in the solid state.

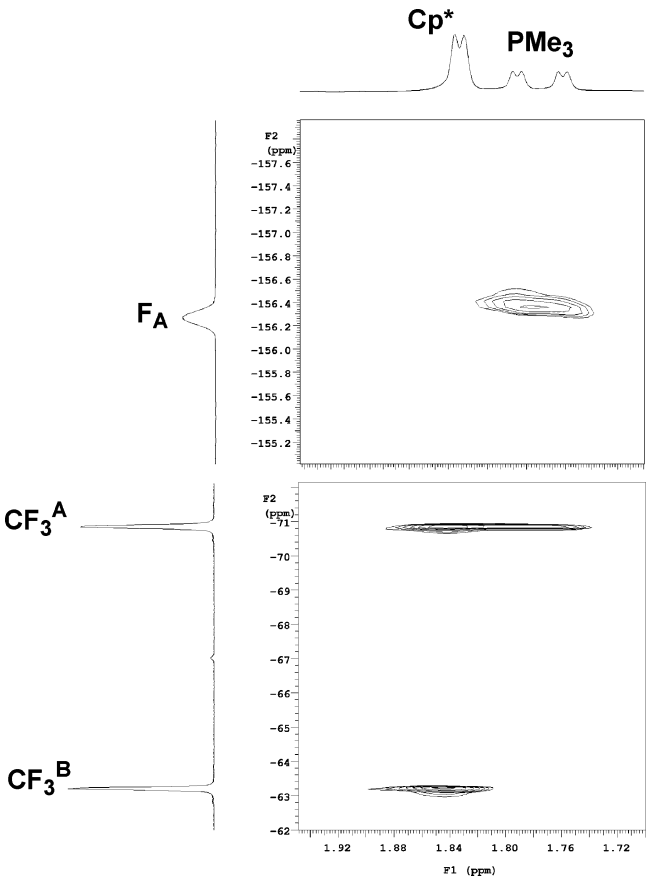

Figure 3. $^{19}F\{^1H\}$ HOESY spectrum for **1** in C_6D_6 solution: mixing time 2.4 s.

Once again, the $^{19}F\{^1H\}$ HOESY results are consistent with the $^{31}P-^{19}F$ coupling pattern observed in the one-dimensional $^{31}P\{^1H\}$ NMR spectrum, in which the PMe_3 appears as a doublet of quartets from coupling to F_A and the closer CF_3^A substituent.

With these promising results in hand, the synthesis and conformational characterization of diastereomeric analogues was attempted. Utilization of perfluoro-*sec*-butyliodide as the sub-

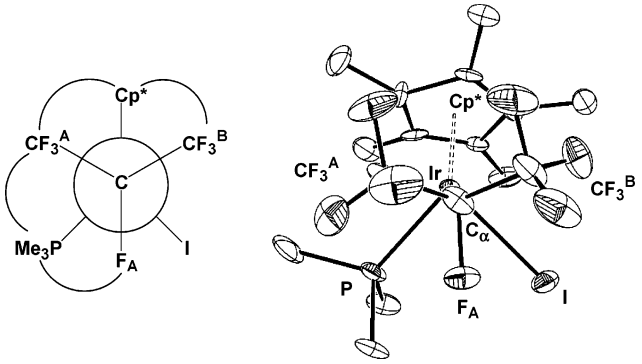

Figure 4. The solution conformation deduced from the $^{19}F\{^1H\}$ HOESY experiment and solid-state structure of **1**. Both are shown as Newman projections down the C−Ir bond. (The curved lines show the observed nOe interactions.)

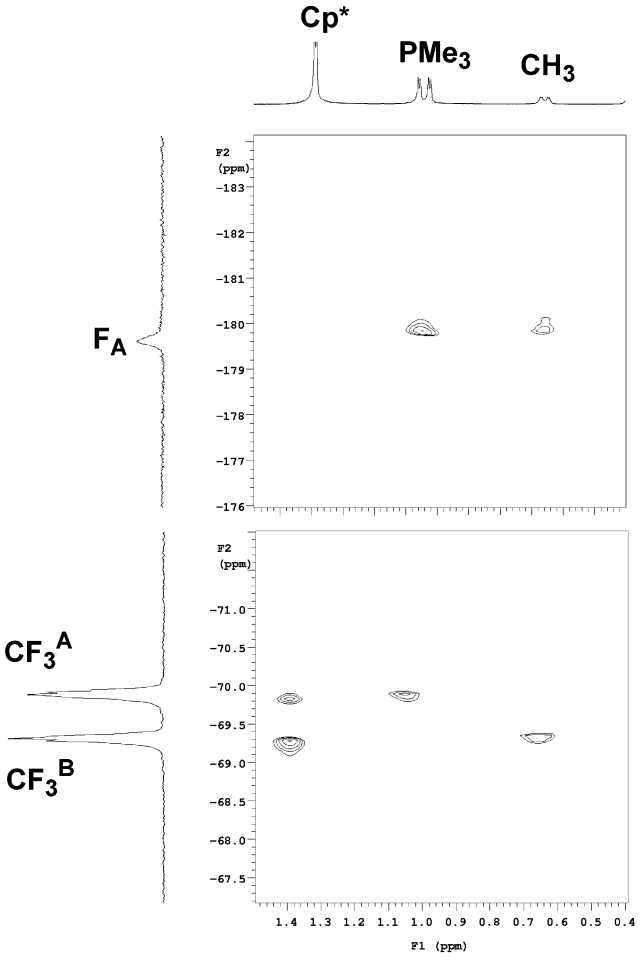

Figure 5. $^{19}F\{^1H\}$ HOESY spectrum for complex **2** in C_6D_6: mixing time 3.0 s.

strate should afford diastereomeric complexes due to the presence of two stereocenters, at Ir and at the α-carbon of the fluoroalkyl ligand.

Oxidative addition of perfluoro-*sec*-butyl iodide [ICF(CF_3)(CF_2CF_3)] to Cp*Ir($CO)_2$ proceeds rapidly at room temperature with displacement of CO, furnishing Cp*Ir(CO)[CF(CF_3)(C_2F_5)]I (**3**) as a ∼2.5:1 mixture of two diastereomers. Epimerization is fairly slow for **3** at room temperature, reaching a ∼7.2:1 equilibrium ratio after more than a week at room temperature. The substitution reaction of **3** with PMe_3 occurs in refluxing toluene within a few hours to give Cp*Ir-

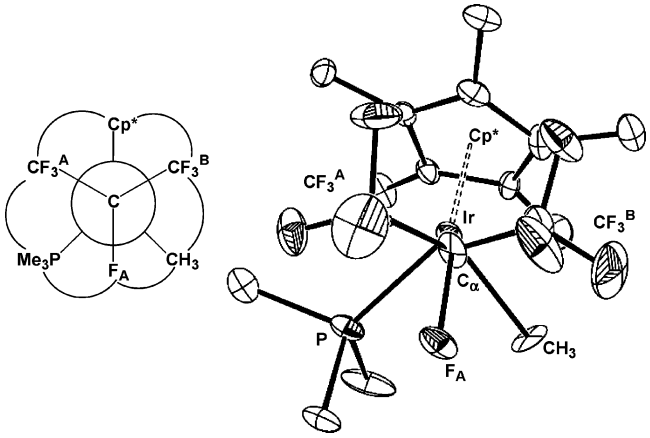

Figure 6. The solution conformation of **2** deduced from the $^{19}F\{^1H\}$ HOESY experiment and the solid-state structure of **2**. (The curved lines show the observed nOe interactions.)

(PMe_3)[CF(CF_3)(CF_2CF_3)]I (**4**), as a ∼5:1 mixture of two diastereomers. The diastereomer ratio varies with the refluxing time, indicating that under these conditions **4** has a configurationally labile metal center, inversion at which results in epimerization of the two diastereomers.

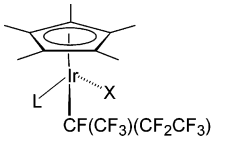

3. X = I; L = CO
4. X = I; L = PMe_3
5. X = CH_3; L = PMe_3

The carbonyl complex **3** has been characterized by IR and NMR spectroscopy, although no diastereomer separation was attempted. The coordinated CO in both diastereomers gives rise to a strong band at 2047 cm^{-1} in the IR spectrum. Each diastereomer of **3** displays a characteristic Cp* peak in the ^1H NMR spectrum, and, in the ^{19}F NMR spectrum ($CDCl_3$), two sets of ^{19}F resonances in a ratio of ∼2.5:1 for the *sec*-C_4F_9 moiety of **3** are observed. The major diastereomer of **3** exhibits two strongly coupled resonances at −87.1 and −113.3 ppm due to the diastereotopic geminal fluorines of the CF_2 group. The $CF_3{}^A$, $CF_3{}^B$, and the α-F_A of the major diastereomer appear as three broad singlets at −67.1, −79.3, and −156.1 ppm, respectively. Similarly, the CF_2 group of the minor diastereomer appears as two broad doublets at −90.1 and −111.0 ppm. The corresponding $CF_3{}^A$, $CF_3{}^B$, and α-F_A appear as three singlets at −66.5, −78.8, and −162.0 ppm, respectively. The coupling patterns for the resonances in the ^{19}F NMR spectrum cannot be fully resolved due to the broadness of the signals. However, the presence of the *sec*-C_4F_9 moiety is unambiguously identifiable from the chemical shifts and integration values.

Diastereomeric PMe_3 complexes **4** were also unambiguously characterized by NMR spectroscopy. Both diastereomers of **4** show characteristic Cp* and PMe_3 peaks in the ^1H NMR spectrum. Interestingly, the PMe_3 signal of the major diastereomer appears as a doublet of doublets from coupling to ^{31}P and the α-F_A, whereas that of the minor diastereomer resonates as a doublet of doublet of doublets from coupling to ^{31}P, the α-F_A,

and one of the geminal fluorines of the CF_2 group. In the ^{19}F NMR spectrum (CD_2Cl_2), the major diastereomer of **4** exhibits strongly coupled resonances at −79.0 and −113.6 ppm due to the CF_2, with the higher field resonance appearing as a doublet of quartets of doublets from coupling with the other geminal fluorine, CF_3^A, and the α-F_A. The CF_3^A appears as a doublet of doublet of quartet of doublets at −69.0 ppm from coupling with one of the higher field CF_2 resonances, the α-F_A, the CF_3^B, and also ^{31}P. The CF_3^B resonates at −79.5 ppm as a doublet of quartet of doublets from coupling with the α-F_A, CF_3^A, and the lower field CF_2 fluorine. The α-F_A resonates at −162.2 ppm as a complicated multiplet due to coupling to eight other fluorines, nine protons from PMe_3, and ^{31}P. The corresponding $^{31}P\{^1H\}$ spectrum exhibits a doublet of quartets at −40.6 ppm from coupling with the α-F_A and CF_3^A. These data, particularly those involving the coupling between CF_3^A and ^{31}P, strongly suggest that the conformation of the major diastereomer is one in which CF_3^A occupies the spatial zone near PMe_3.

For the minor diastereomer of **4**, the $^{31}P\{^1H\}$ spectrum exhibits a doublet of doublets at −41.1 ppm from coupling to one of the lower field CF_2 fluorines and the α-F_A. The corresponding lower field CF_2 fluorine appears as a doublet of doublet of doublet of decets from coupling with the other geminal fluorine, ^{31}P, α-F_A, and nine protons from PMe_3. The other geminal fluorine appears as a doublet of quartet of doublets due to the geminal coupling and also the couplings with the CF_3^A and the α-F_A. The CF_3^B appears at −78.8 ppm as a doublet of quartets from coupling with the α-F_A and CF_3^A, which appear as broad peaks at −157.4 and −61.3 ppm. No coupling is observed between CF_3^A and ^{31}P, suggesting that, in the minor diastereomer, this CF_3^A lies in the zone opposite to PMe_3, an observation complemented by observation of coupling between ^{31}P and one of the CF_2 fluorines.

The relative configurations of the major diastereomers of **3** and **4** have been determined by correlation of their ^{19}F NMR spectra with their X-ray crystal structures. ORTEP views of the molecular structures of **3** and **4** are shown in Figures 7 and 8, respectively. The NMR correlation experiment was done by dissolving the same crystal mounted for X-ray diffraction data collection in a minimum amount of a deuterated solvent at −75 °C and recording the ^{19}F NMR spectrum at −75 °C for several hours to obtain a satisfactory signal. The samples were then allowed to warm to room temperature. In the case of **4**, the ^{19}F NMR spectrum showed one set of ^{19}F resonances corresponding to the major diastereomer of **4**. In the case of **3**, the ^{19}F NMR spectrum was initially only that of the major diastereomer, with the gradual appearance of signals corresponding to the minor diastereomer over time at room temperature, indicating that epimerization at the iridium center for **3** was faster than that of **4**. Consequently, for both **3** and **4**, the crystallographic determinations show that the major diastereomers have (S_{Ir}, S_C) or (R_{Ir}, R_C) relative configurations at the metal center and the α-carbon, respectively, with the minor diastereomers in each case adopting (R_{Ir}, S_C) or (S_{Ir}, R_C) relative configurations. To define the relative configuration at the iridium center, Cp* is arbitrarily treated as an atom with a C5 (60) molecular weight.[30] Every NMR resonance corresponding to each diastereomer is thereby defined unambiguously.

In the solid state, the major diastereomer of **3** adopts a conformation in which the CF_2CF_3 group is eclipsed with the CO ligand, the α-CF_3 is close to the iodide, and the α-fluorine is close to the Cp*, as shown in Figure 5. This conformation is almost identical to that found in the perfluoro-iso-propyl analogue Cp*Ir[$CF(CF_3)_2$](CO)I.[29] In contrast, the major diastereomer of **4** adopts a staggered conformation in the solid state, as found for its perfluoro-iso-propyl analogue **1**.[29]

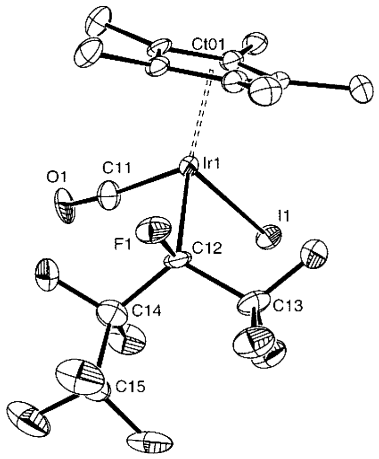

Figure 7. ORTEP diagram of the non-hydrogen atoms of the major diastereomer of **3**, showing the partial atom-labeling scheme. Thermal ellipsoids are shown at the 30% level. Selected bond lengths (Å) and angles (deg): Ir(1)−C(11), 1.876(10); Ir(1)−C(12), 2.144(9); Ir(1)−Ct01, 1.8677(4); Ir(1)−I(1), 2.7018(7); C(11)−O(1), 1.053(12); C(12)−F(1), 1.431(11); Ct01−Ir(1)−C(11), 125.7(4); Ct01−Ir(1)−C(12), 124.5(3); Ct01−Ir(1)−I(1), 120.37(2); C(11)−Ir(1)−C(12), 93.2(4); C(11)−Ir(1)−I(1), 87.9(3); C(12)−Ir(1)−I(1), 96.0(3); Ir(1)−C(12)−C(13), 115.2(7); Ir(1)−C(12)−C(14), 115.3(7); Ir(1)−C(12)−F(1), 107.9(6); C(13)−C(12)−C(14), 113.1(9).

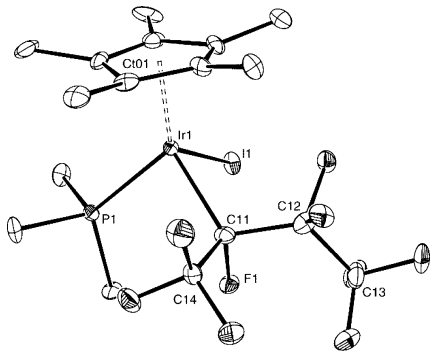

Figure 8. ORTEP diagram of the non-hydrogen atoms of the major diastereomer of **4**, showing the partial atom-labeling scheme. Thermal ellipsoids are shown at the 30% level. Selected bond lengths (Å) and angles (deg): Ir(1)−C(11), 2.150(12); Ir(1)−Ct01, 1.881(10); Ir(1)−I(1), 2.7026(8); Ir(1)−P(1), 2.296(3); C(11)−F(1), 1.404(11); Ct01−Ir(1)−C(11), 130.8(8); Ct01−Ir(1)−I(1), 119.1(7); Ct01−Ir(1)−P(1), 126.2(8); C(11)−Ir(1)−I(1), 89.3(3); C(11)−Ir(1)−P(1), 91.9(3); P(1)−Ir(1)−I(1), 86.83(7); Ir(1)−C(11)−C(12), 114.7(8); Ir(1)−C(11)−C(14), 115.3(7); Ir(1)−C(11)−F(1), 112.5(7); C(12)−C(11)−C(14), 109.2(10).

This correlation of diastereomer configuration with NMR resonances is a classic method, but one which is dependent upon obtaining satisfactory crystals for an X-ray structural determination, and a direct NMR correlation experiment in which the stereochemical integrity of the stereocenter at the metal is not compromised during the time course of the experiment. The dangers associated with some attempted correlations are well established.[30,31] Furthermore, while such correlations may

(30) Brunner, H. *Angew. Chem., Int. Ed.* **1999**, *38*, 1194−1208.
(31) Brunner, H. *Eur. J. Inorg. Chem.* **2001**, 905−912.

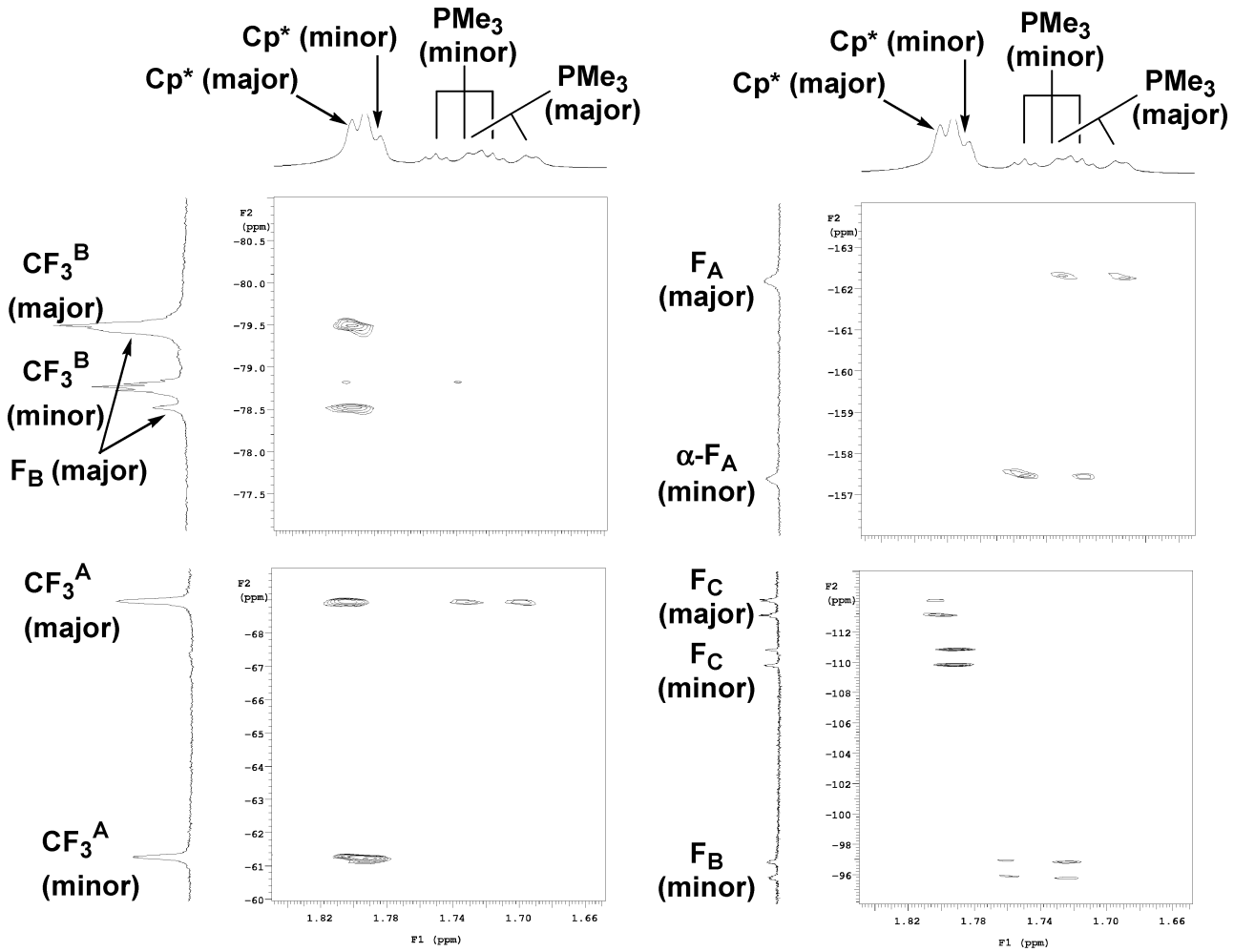

Figure 9. $^{19}F\{^1H\}$ HOESY spectrum for the diastereomers of **4** in C_6D_6: mixing time 3.0 s.

confirm the relative configurational relationships between stereocenters, they have nothing unambiguous to say about solution conformations, which may be different from that observed in the crystal. The data described already suggest that the presence or absence of $^{19}F-^{31}P$ coupling is capable of distinguishing which groups are close in space to ^{31}P, but such data may not always be available, and we sought further confirmation of the solution conformations of each diastereomer of **4** using HOESY techniques.

The $^{19}F\{^1H\}$ HOESY spectrum of a mixture of the diastereomers of **4** is shown in Figure 9. Assignment of the conformations is straightforward. In the major diastereomer of **4**, $CF_3{}^A$ is close to PMe_3 and Cp*; F_B, F_C, and $CF_3{}^B$ are close to Cp* only; F_A is close in space to PMe_3 only. Cross-peaks for the minor diastereomer are complementary and illustrate that $CF_3{}^A$ is close to Cp* but not to PMe_3; and F_A is close to PMe_3 only. More detail is provided in the $^{19}F\{^1H\}$ HOESY spectrum of a sample of **4** containing predominantly the major diastereomer, shown in Figure 10, along with the deduced solution-state conformation and the corresponding solid-state structure, each viewed along the α-C_F-Ir bond. Once again, the conclusion is clear, that the solution conformation of the major diastereomer is the same as that observed in the solid state, and that of the minor diastereomer involves switching the locations of $CF_3{}^A$ and the CF_2CF_3 substituents of the fluorocarbon ligand as shown in Figure 11.

The doublet of quartets coupling pattern in the one-dimensional $^{31}P\{^1H\}$ NMR spectrum of the major diastereomer of **4** also lends credibility to the solution-state structure determined by HOESY: clearly, the splitting pattern is due to ^{31}P coupling to $CF_3{}^A$ and F_A, which occupy zones adjacent to the PMe_3 ligand. Similarly, the one-dimensional $^{31}P\{^1H\}$ NMR spectrum for the minor diastereomer also agrees with the solution-state structure determined by the $^{19}F\{^1H\}$ HOESY data: the doublet of doublets is the result of ^{31}P coupling to F_A and F_B.

Overall, the $^{19}F\{^1H\}$ HOESY data for the major and minor diastereomers of compound **4** are mutually consistent. As a final test, the $^{19}F\{^1H\}$ HOESY technique was applied to the determination of the solution conformation and relative configurations of $Cp^*Ir(PMe_3)[CF(CF_3)(C_2F_5)]CH_3$ (**5**), for which crystals suitable for X-ray diffraction could not be obtained.

The methyl compound **5** was synthesized in quantitative yields as a 1.7:1 mixture of two diastereomers by reaction of the triflate precursor $Cp^*Ir[CF(CF_3)(C_2F_5)](PMe_3)OTf$ and $Cp_2Zr(CH_3)_2$. As expected, **5** displays two sets of characteristic Cp*, PMe_3, and CH_3 resonances in the ^1H NMR spectrum, two sets of ^{19}F resonances, and two ^{31}P resonances, corresponding to the two diastereomers. The CH_3 resonance of the major diastereomer appears as a doublet of quartets from coupling with ^{31}P and $CF_3{}^A$, while that of the minor diastereomer appears as a doublet of doublets from coupling with ^{31}P and one of the geminal fluorines. The PMe_3 resonance of the major diastere-

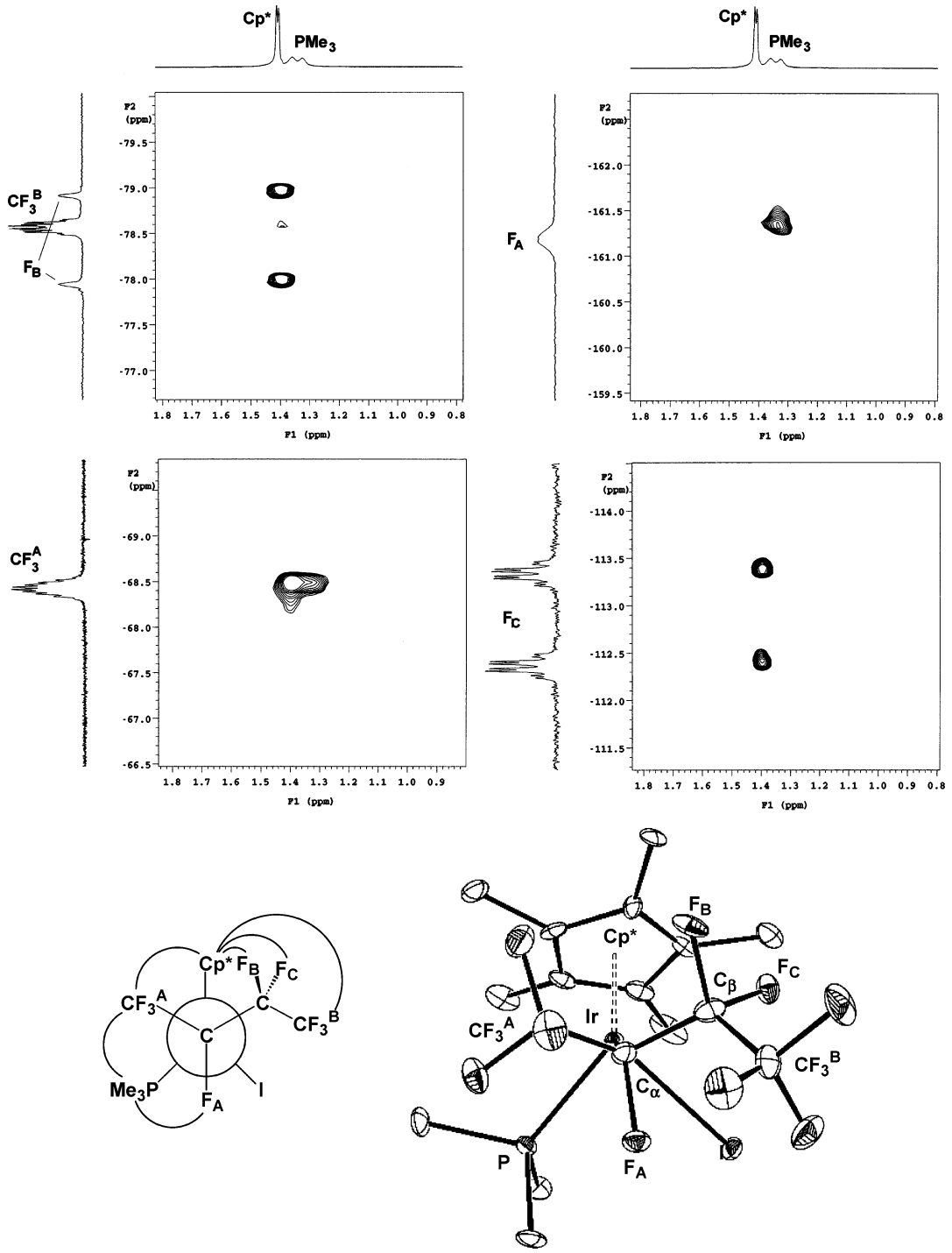

Figure 10. $^{19}F\{^{1}H\}$ HOESY spectrum (C_6D_6: mixing time 3.0 s) of the major diastereomer of **4**, the deduced solution conformation, and the corresponding solid-state structure. (The curved lines show the observed NOE interactions.)

omer appears as a doublet of doublet of doublets from coupling with ^{31}P, the F_A, and one of the geminal fluorines of the CF_2, while the corresponding resonance for the minor diastereomer appears as a doublet of doublets from coupling with ^{31}P and F_A. Likewise, the $^{31}P\{^{1}H\}$ spectrum of the major diastereomer exhibits a doublet of doublets from coupling with F_A and one of the geminal fluorines, and the corresponding resonance for the minor diastereomer exhibits a doublet of quartets from coupling with α-F_A and $CF_3{}^A$. Based on the observations outlined above, these data alone strongly suggest that the configuration for the major diastereomer of **5** is the same as that for the minor diastereomer of **4**.

The $^{19}F\{^{1}H\}$ HOESY spectrum for the two diastereomers of **5** is shown in Figure 12. Once again, assignment of conformation and relative configuration is straightforward. In the major diastereomer, $CF_3{}^A$ is close to both Cp* and CH_3 but not to PMe_3; F_A is close in space to PMe_3 and CH_3; $CF_3{}^B$ and the geminal fluorines F_B and F_C are close to Cp* and PMe_3. Cross-peaks for the minor diastereomer show that $CF_3{}^A$ is close to both Cp* and PMe_3 but not to CH_3; F_A is close in space to

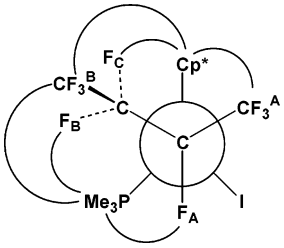

Figure 11. The solution conformation of the minor diastereomer of **4** deduced from the $^{19}F\{^1H\}$ HOESY experiment. (The curved lines show the observed NOE interactions.)

PMe_3 and CH_3; F_C is close to Cp*, and F_B is close to both Cp* and CH_3; $CF_3{}^B$ is close to Cp* and to the CH_3.

Accordingly, the solution-state conformations for both diastereomers of **5** are clear from those nOe interactions; Newman projections viewed along the α-C_F−Ir bond are shown in Figure 13. The major diastereomer of **5** has the (S_{Ir}, R_C) or (R_{Ir}, S_C) relative configuration, while the minor diastereomer has the (S_{Ir}, S_C) or (R_{Ir}, R_C) relative configuration, that is, the opposite configurations from those of the major and minor diastereomers of **4**. This is a result that would be unobtainable by any other technique without suitable crystals, and it illustrates the power of HOESY in these kinds of molecules.

In summary, the $^{19}F\{^1H\}$ HOESY technique is a powerful tool in establishing the solution conformations and relative configurations of iridium−fluoroalkyl complexes. It provides a powerful complementary alternative method to X-ray crystallography for determining the relative configuration of diastereomers in these kinds of compounds. In the case of iridium(III) complexes bearing perfluoro-iso-propyl and perfluoro-*sec*-butyl ligands, the solution conformations are in good agreement with their solid-state structures. We now feel confident in using this technique for the determination of solution structural information in these and related compounds, and we will report our findings in due course.

Experimental Section

General Considerations. All reactions were performed in oven-dried glassware, using standard Schlenk techniques, under an atmosphere of nitrogen which has been deoxygenated over BASF catalyst and dried over Aquasorb, or in a Braun Drybox. Methylene chloride, hexane, diethyl ether, and toluene were dried over an alumina column under nitrogen.[32] Benzene was distilled under nitrogen from potassium benzophenone ketyl. IR spectra were recorded on a Perkin-Elmer FTIR 1600 Series spectrometer. NMR spectra were recorded on a Varian Unity Plus 300 FT spectrometer. ^1H NMR spectra were referenced to the protio impurity in the solvent: C_6D_6 (7.16 ppm), $CDCl_3$ (7.27 ppm), CD_2Cl_2 (5.32 ppm). ^{19}F NMR spectra were referenced to external $CFCl_3$ (0.00 ppm). $^{31}P\{^1H\}$ NMR spectra were referenced to external 85% H_3PO_4 (0.00 ppm). Cp*Ir(PMe_3)[$CF(CF_3)_2$]I (**1**) was prepared as previously described.[29]

Prior to the acquisition of $^1H\{^{19}F\}$ HOESY spectra, PW90° (irradiation power for the 90° pulse) and T_1 for both ^1H and ^{19}F were measured. The mixing time was set to be the longest T_1 of any protons or fluorines in the complex. Specific mixing times are given in each figure caption. The delay time was set as 1.3 times the longest T_1.

Cp*Ir(PMe_3)[$CF(CF_3)_2$](OTf). A solution of Cp*Ir(PMe_3)[$CF(CF_3)_2$]I (100 mg, 0.143 mmol) in CH_2Cl_2 (5 mL) was added slowly to a slurry of AgOTf (44.1 mg, 0.172 mmol) in CH_2Cl_2 (5 mL). The reaction mixture was stirred for 30 min and then filtered to give a yellow solution. The solvent was removed under vacuum, and the residue was extracted into toluene to give a yellow solution, which was filtered through a cannula under N_2. The toluene filtrate was concentrated, and hexane was added to precipitate the yellow solid (89 mg, 86%). Anal. Calcd for $C_{17}H_{24}F_{10}IrO_3P$ (721.59): C, 28.29; H, 3.35. Found: C, 28.32; H, 3.37. ^1H NMR ($CDCl_3$): δ 1.72 (dd, $^2J_{PH} = 11$, $^5J_{HF} = 2$, 9H, PMe_3), 1.68 (d, $^4J_{PH} = 2$, 15H, C_5Me_5). ^{19}F NMR ($CDCl_3$): δ −69.57 (br s, 6F, CF_3), 78.58 (s, 3F, OSO_2CF_3), −114.0 (br s, 1F, CF). $^{31}P\{^1H\}$ NMR ($CDCl_3$): δ −19.76 (br s, PMe_3).

Cp*Ir(PMe_3)[$CF(CF_3)_2$](CH_3) (2). (1) From MeLi: Cp*Ir(PMe_3)-[$CF(CF_3)_2$]OTf (30 mg, 0.0415 mmol) was partially dissolved in ether (0.5 mL), and the solution was freeze−pump−thawed three times. MeLi/ether (89 μL, 0.125 mmol, 1.4 M, 3 equiv) was added into the cold solution by syringe under N_2. The reaction solution was allowed to warm to room temperature gradually and was stirred for about 10 min. The solution changed from orange yellow to pale yellow. A few drops of methanol were added to quench the excess MeLi. The solution was then pumped down, and the residue was extracted with hexane to give a yellow solution. Evaporation of hexane from the yellow solution afforded a pale yellow solid (17.6 mg, 72%).

(2) From $ZnMe_2$: Cp*Ir(PMe_3)[$CF(CF_3)_2$]OTf (100 mg, 0.138 mmol) was partially dissolved in toluene (0.5 mL), and the solution was freeze−pump−thawed three times. $ZnMe_2$/toluene (69 μL, 0.138 mmol, 2 M, 1 equiv) was added into the cold solution by syringe under N_2.The reaction solution was allowed to warm to room temperature gradually and stirred for half an hour. A few drops of methanol were added to quench the excess $ZnMe_2$. The solution was then pumped down, and the residue was extracted with hexane to give a pale yellow solution. Evaporation of hexane afforded a pale yellow solid (65 mg, 80%).

(3) From Cp_2ZrMe_2: A toluene (20 mL) solution of Cp*Ir(PMe_3)-[$CF(CF_3)_2$]OTf (15 mg, 0.0208 mmol) and $ZrCp_2(CH_3)_2$ (2.62 mg, 0.0104 mmol, 0.5 equiv) was stirred at room temperature for 1 h under N_2. The solvent was evaporated, and the residue was extracted into hexane. Removal of hexane under vacuum gave an off-white solid (12.2 mg, 86%). Anal. Calcd for $C_{17}H_{27}F_7IrP$ (587.58): C, 34.75; H, 4.63. Found: C, 34.74; H, 4.60. ^1H NMR (C_6D_6): δ 1.39 (d, $^4J_{HP} = 2$, 15H, C_5Me_5), 1.04 (dd, $^2J_{HP} = 10$, $^5J_{HF} = 2$, 9H, PMe_3), 0.66 (dqd, $^3J_{HP} = 7$, $^5J_{HF} = 2$, $^4J_{HF} = 0.9$, 3H, CH_3). ^{19}F NMR (C_6D_6): δ −69.3 (dq, $^3J_{FF} = 10$, $^4J_{FF} = 10$, 3F, CF_3), −69.9 (dqdq, $^3J_{FF} = 10$, $^4J_{FF} = 10$, $^4J_{PF} = 7$, $^5J_{HF} = 2$, 3F, CF_3), −179.6 (br s, 1F, CF). $^{31}P\{^1H\}$ NMR (C_6D_6): δ −38.4 (dq, $^3J_{PF} = 11$, $^4J_{PF} = 7$, PMe_3).

Cp*Ir(CO)[$CF(CF_3)(CF_2CF_3)$]I (3). Cp*Ir$(CO)_2$ (100 mg, 0.261 mmol) was dissolved in CH_2Cl_2 (20 mL), and $ICF(CF_3)(CF_2CF_3)$ (99 μL, 0.287 mmol) was added by syringe under nitrogen. The yellow solution changed to orange and was stirred for 1.5 h. The solvent was removed under vacuum to give an orange powder (165 mg, 90%). The NMR spectra show the product is formed as two diastereomers in a 2.5:1 ratio. The compound can be recrystallized from CH_2Cl_2/hexane. IR (CH_2Cl_2): $\nu_{co} = 2047$ cm^{-1}. Anal. Calcd for $C_{15}H_{15}F_9IIrO$ (701.39): C, 25.69; H, 2.16. Found: C, 25.46; H, 2.07.

The major diastereomer, ^1H NMR ($CDCl_3$): δ 2.08 (s, 15H, Cp*). ^{19}F NMR ($CDCl_3$): δ −67.1 (s, 3F, $CF_3{}^A$), −79.3 (s, 3F, $CF_3{}^B$), −87.1 (d, $^2J_{FF} = 289$, 1F, CF_2), −113.3 (d, $^2J_{FF} = 289$, 1F, CF_2), −156.1 (br s, 1F, F_A).

The minor diastereomer, ^1H NMR ($CDCl_3$): δ 2.08 (s, 15H, Cp*). ^{19}F NMR ($CDCl_3$): δ −66.5 (s, 3F, $CF_3{}^A$), −78.8 (s, 3F, $CF_3{}^B$), −90.0 (br d, $^2J_{FF} = 277$, 1F, CF_2), −111.0 (d, $^2J_{FF} = 277$, 1F, CF_2), −162.0 (br s, F_A).

Cp*Ir(PMe_3)[$CF(CF_3)(CF_2CF_3)$]I (4). Cp*Ir[$CF(CF_3)(C_2F_5)$](CO)I (160 mg, 0.228 mmol) was dissolved in toluene (15 mL). The solution was freeze−pump−thawed three times, and PMe_3 (30.7 μL, 0.297 mmol) was added by syringe under nitrogen. The reaction was heated at reflux under nitrogen for 2 h, and the volatiles were removed under vacuum to give a yellow solid, which was washed with hexane and

(32) Pangborn, A. B.; Giardello, M. A.; Grubbs, R. H.; Rosen, R. K.; Timmers, F. J. *Organometallics* **1996**, *15*, 1518−1520.

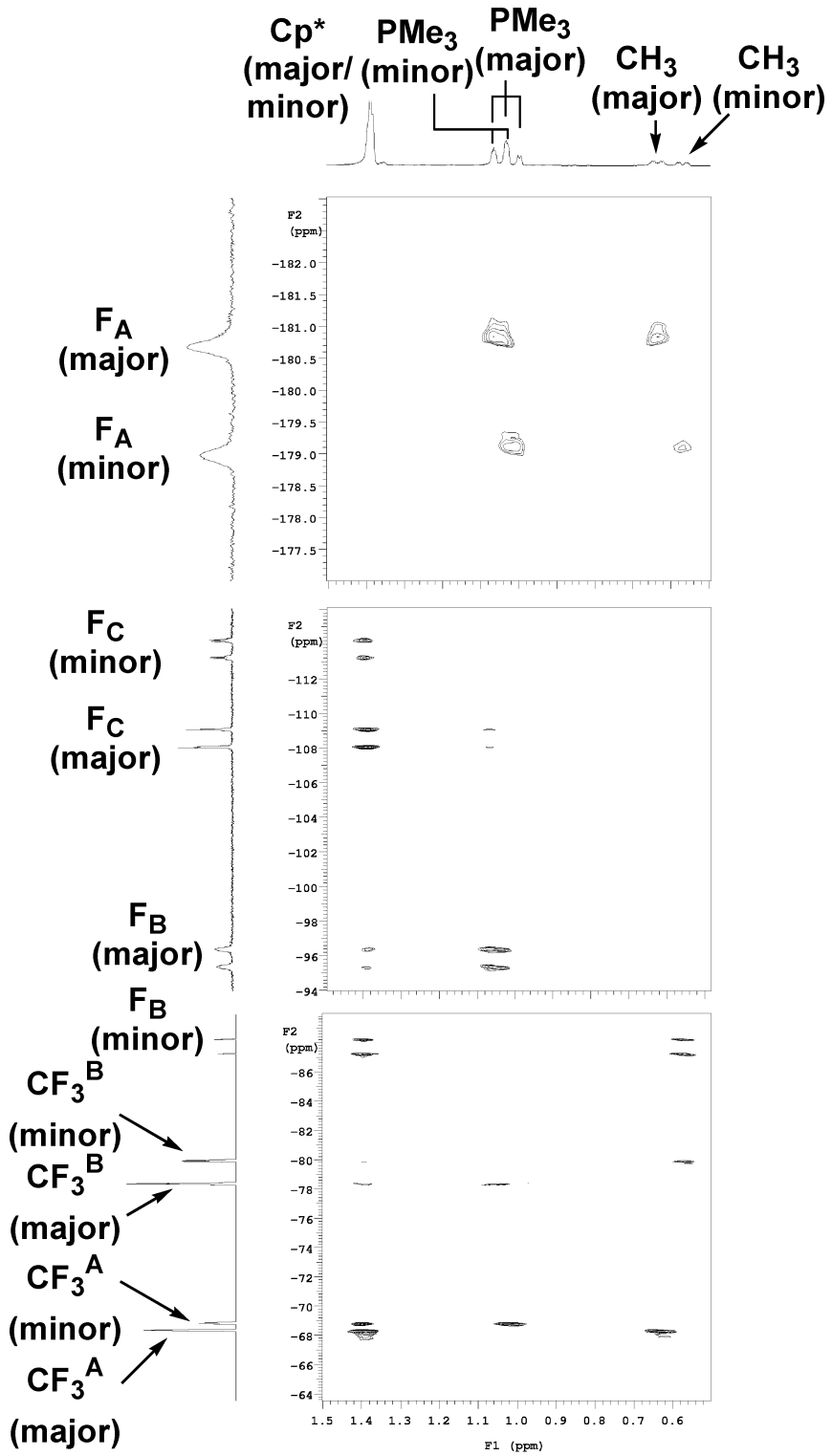

Figure 12. $^{19}F\{^1H\}$ HOESY spectrum for the two diastereomers of **5** in C_6D_6: mixing time 2.4 s.

dried under vacuum, affording the product in 92% yield (157 mg). The NMR spectra show the product is formed as two diastereomers in a ~5:1 ratio. The compound can be recrystallized from CH_2Cl_2/hexane. Anal. Calcd for $C_{17}H_{24}F_9IIrP$ (749.46): C, 27.24; H, 3.23. Found: C, 27.28; H, 3.12.

The major diastereomer, ^1H NMR (C_6D_6): δ 1.40 (d, $^4J_{HP} = 2$, 15H, Cp*), 1.33 (d, $^2J_{HP} = 10$, 9H, PMe_3). ^{19}F NMR (C_6D_6): δ −68.5 (ddqd, $^4J_{FF} = 21$, $^3J_{FF} = 15$, $^5J_{FF} = 8$, $^4J_{PF} = 8$, 3F, CF_3^A), −78.5 (br d, $^2J_{FF} = 265$, 1F, CF_2), −78.6 (dqd, $^4J_{FF} = 20$, $^5J_{FF} = 8$, $^3J_{FF} = 3$, 3F, CF_3^B), −112.9 (dqd, $^2J_{FF} = 265$, $^4J_{FF} = 21$, $^3J_{FF} = 7$, 1F, CF_2), −161.2 (br s, 1F, F_A). $^{31}P\{^1H\}$ NMR (C_6D_6): δ −40.6 (dq, $^3J_{PF} = 10$, $^4J_{PF} = 8$, PMe_3).

The minor diastereomer, ^1H NMR (C_6D_6): δ 1.40 (d, $^4J_{HP} = 2$, 15H, Cp*), 1.33 (d, $^2J_{HP} = 11$, 9H, PMe_3). ^{19}F NMR (C_6D_6): δ −60.6 (br s, 3F, CF_3^A), −78.0 (br s, 3F, CF_3^B), −96 (d, $^2J_{FF} = 289$, 1F, CF_2), −110.0 (br d, $^2J_{FF} = 289$, 1F, CF_2), −156.4 (br s, 1F, F_A). $^{31}P\{^1H\}$ NMR (C_6D_6): δ −42.0 (dd, $^4J_{PF} = 36$, $^3J_{PF} = 8$, PMe_3).

$Cp^*Ir(PMe_3)[CF(CF_3)CF_2CF_3]OTf$. $Cp^*Ir[CF(CF_3)(C_2F_5)](PMe_3)I$ (116 mg, 0.15 mmol) was dissolved in toluene (10 mL) and was added into an AgOTf (41.9 mg, 0.16 mmol)/toluene (10 mL) slurry dropwise.

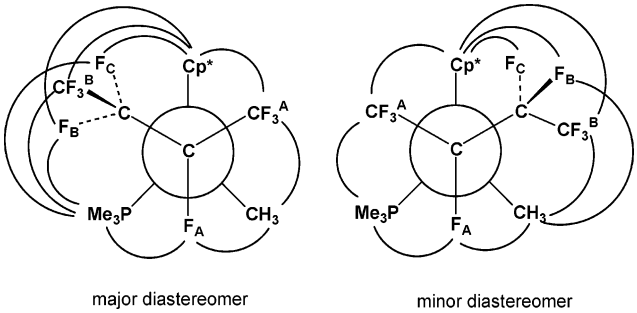

Figure 13. The solution conformations of the two diastereomers of **5** deduced from $^{19}F\{^1H\}$ HOESY experiment. (The curved lines show the observed NOE interactions.)

The solution was stirred for 30 min and was filtered under N_2 to give a yellow solution. The solution was concentrated, and hexane was added to precipitate a yellow solid (116 mg, 96%). ^1H NMR (C_6D_6): δ 1.24 (dd, $^2J_{HP} = 11$, $^5J_{HF} = 3$, 9H, PMe_3), 1.14 (d, $^2J_{HP} = 2$, 15H, C_5Me_5). ^{19}F NMR (C_6D_6): δ −67.8 (s, 3F, CF_3^A), −77.9 (s, 3F, SO_3CF_3), 79.5 (br s, 3F, CF_3^B), −91.3 (br d, $^2J_{FF} = 283$, 1F, CF_2), −112.7 (br d, $^2J_{FF} = 265$, 1F, CF_2), −180.1 (br s, 1F, F_A). $^{31}P\{^1H\}$ NMR (C_6D_6): δ −22.8 (br d, $^3J_{PF} = 19$, PMe_3).

$Cp^*Ir(PMe_3)[CF(CF_3)CF_2CF_3]CH_3$ (5). A toluene (20 mL) solution of $Cp^*Ir(PMe_3)[CF(CF_3)(C_2F_5)]OTf$ (50 mg, 0.065 mmol) and $Cp_2Zr(CH_3)_2$ (16.3 mg, 0.065 mmol, 1 equiv) was stirred at room temperature for 1 h under N_2. The solvent was removed on a rotary evaporator, and the residue was extracted into hexane. Removal of hexane under vacuum gave a white solid as a 1.7:1 mixture of two diastereomers, which was recrystallized from hexanes (34 mg, 83%). Anal. Calcd for $C_{18}H_{27}F_9IrP$ (637.59): C, 33.91; H, 4.27. Found: C, 33.54; H, 3.89.

The major diastereomer, ^1H NMR (C_6D_6): δ 1.39 (d, $^4J_{HP} = 2$, 15H, C_5Me_5), 1.05 (ddd, $^2J_{HP} = 10$, $^5J_{HF} = 1$, $^5J_{HF} = 1$, 9H, PMe_3), 0.64 (dq, $^3J_{HP} = 7$, $^5J_{HF} = 2$, 3H, CH_3). ^{19}F NMR (C_6D_6): δ −68.4 (qdddq, $^5J_{FF} = 11$, $^4J_{FF} = 9$, $^3J_{FF} = 9$, $^6J_{HF} = 2$, 3F, CF_3^A), −78.6 (dq, $^4J_{FF} = 11$, $^5J_{FF} = 11$, 3F, CF_3^B), −96.0 (br dd, $^2J_{FF} = 288$, $^4J_{PF} = 8$, 1F, CF_2), −108.6 (ddq, $^2J_{FF} = 288$, $^3J_{FF} = 9$, $^4J_{FF} = 9$, 1F, CF_2), −180.8 (br s, 1F, F_A). $^{31}P\{^1H\}$ NMR (C_6D_6): δ −39.0 (dd, $^3J_{PF} = 30$, $^4J_{PF} = 8$, PMe_3).

The minor diastereomer, ^1H NMR (C_6D_6): δ 1.39 (d, $^4J_{HP} = 2$, 15H, C_5Me_5), 1.01 (dd, $^2J_{HP} = 10$, $^5J_{HF} = 2$, 9H, PMe_3), 0.57 (dd, $^3J_{HP} = 6$, $^5J_{HF} = 2$, 3H, CH_3). ^{19}F NMR (C_6D_6): δ −68.9 (ddqd, $^4J_{FF} = 20$, $^3J_{FF} = 13$, $^5J_{FF} = 8$, $^4J_{PF} = 6$, 3F, CF_3^A), −80.0 (dq, $^4J_{FF} = 21$, $^5J_{FF} = 8$, 3F, CF_3^B), −87.7 (br d, $^2J_{FF} = 279$, 1F, CF_2), −113.8 (dqd, $^2J_{FF} = 279$, $^4J_{FF} = 20$, $^3J_{FF} = 7$, 1F, CF_2), −179.0 (br s, 1F, F_A). $^{31}P\{^1H\}$ NMR (C_6D_6): δ −36.5 (dq, $^3J_{PF} = 6$, $^4J_{PF} = 6$, PMe_3).

X-ray Crystal Structure Determinations. Diffraction intensity data were collected with Bruker Smart Apex CCD (**2**) and Siemens P4 CCD (**3**,**4**) diffractometers. Crystal, data collection, and refinement parameters are given in Table 1. The structures were solved using the Patterson function, completed by subsequent difference Fourier syntheses, and refined by full matrix least-squares procedures on F^2. SADABS absorption corrections were applied to all structures. In all structures, all non-hydrogen atoms were refined with anisotropic displacement coefficients, and hydrogen atoms were treated as idealized contributions. The Flack parameters for noncentrosymmetrical structures **2** and **4** are 0.10(2) and 0.034(9), respectively. All software and sources of scattering factors are contained in the SHELXTL (5.10) program package (G. Sheldrick, Bruker XRD, Madison, WI).

Acknowledgment. This work is dedicated to Professor Walter H. Stockmayer, an inspirational colleague, teacher, and expert on the conformational properties of fluorinated chains, on the occasion of his 90th birthday. R.P.H. is grateful to the National Science Foundation for generous research support.

Supporting Information Available: Crystallographic information files (CIF) for compounds **2**, **3**, and **4**. This material is available free of charge via the Internet at http://pubs.acs.org.

JA049225Q